X-513-65-43

NASA TM X-55436

UNIFIED S-BAND 30-FOOT ANTENNA SIDE LOBE RADIATION

GPO PRICE $ _____

CFSTI PRICE(S) $ _____

Hard copy (HC) 2.00

Microfiche (MF) .50

ff 653 July 65

BY

J. R. MOORE

FEBRUARY 1965

NASA

GODDARD SPACE FLIGHT CENTER

GREENBELT, MARYLAND

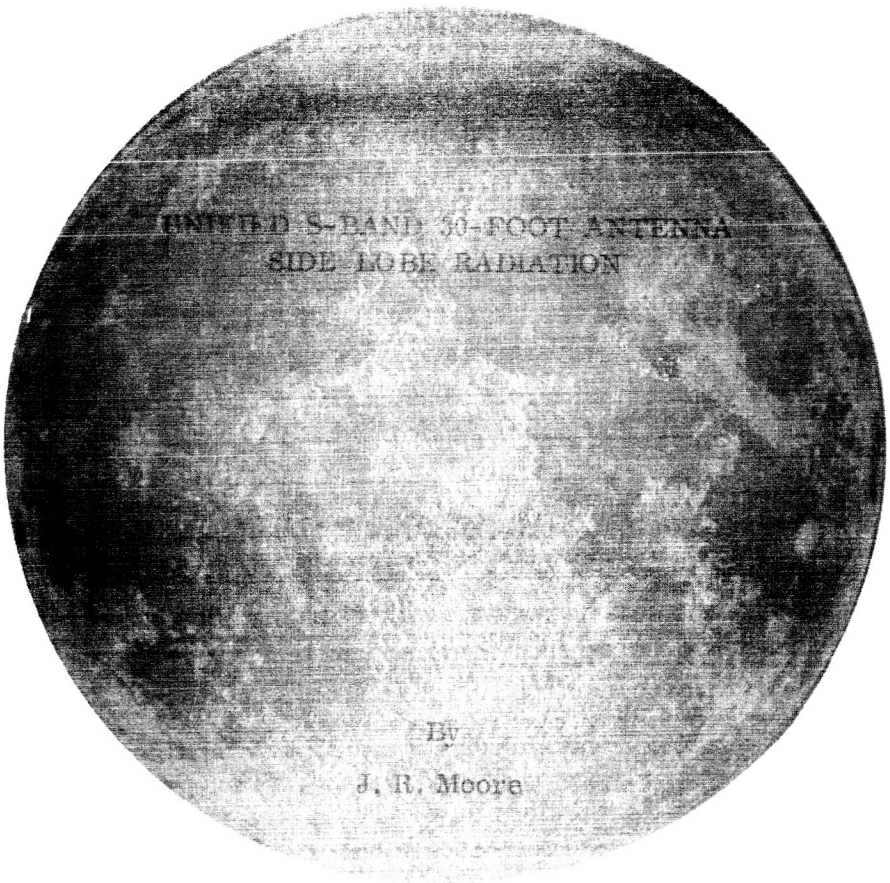

UNTILTED S-BAND 30-FOOT ANTENNA SIDE LOBE RADIATION

By

J. R. Moore

February 1965

Goddard Space Flight Center
Greenbelt, Maryland

UNIFIED S-BAND 30-FOOT ANTENNA SIDE LOBE RADIATION

By
J. R. Moore

2 3615

SUMMARY

Computations have been made to establish an upper bound for the near field side lobe energy density which may be expected from the S-band thirty-foot antennas when transmitting at a power level of ten kilowatts.

The immediate problem is concerned with areas displaced about eight degrees from the axis of the main beam, at ranges of two hundred feet and four hundred feet from the antenna.

The results indicate that an energy density of less than one milliwatt per square centimeter may be expected for angles greater than four degrees off the axis at a distance of four hundred feet and at angles greater than eight degrees off the axis at a range of two hundred feet.

These figures apply to the radiation from the parabolic aperture and do not include possible leakage or indirect radiation.

The computations by the analytical method are made in two steps. First, the relation between the off axis position and a position on the axis at the same range is determined. Then the relation between the on axis position and a similar position in the far field is found. For the first computation, an aperture with uniform illumination is used since this is easier to compute and gives a higher off axis field intensity than the tapered illumination. In the second step, an aperture with tapered illumination is used.

CONTENTS

UNIFIED S-BAND 30-FOOT ANTENNA SIDE LOBE RADIATION

By
J. R. Moore

INTRODUCTION

It is desired to determine the near field intensity created by the 10 KW continuous wave S-Band transmitter, operating with the 30-foot S-Band system at the proposed site in Bermuda. Figure 1 shows the dimensions of the reflecting surfaces as proposed by Collins Radio Company on page II-2-6 of their Report (Reference 6). The field intensity is desired at ranges of 200 and 400 feet from the antenna and at an angular displacement of 8 degrees from the center of the beam. These conditions are imposed by the terrain near the proposed location in Bermuda.

I. METHODS USED FOR THE ANALYSIS

a. Analogue Methods

To prepare initial estimates of the near field intensity, a mathematical analogue was devised. This analogue consisted of a circle which was scaled to the size of the radiating aperture. The circle was divided into ten concentric bands, of equal width, as shown in Figure 2. Each band was coded to indicate the intensity of illumination at its particular radius. Radial lines were also drawn on the circle to divide the rings into incremental areas.

A transparent overlay was then prepared, with scaled concentric circles representing the boundaries of the Fresnel regions at the specified range and wave length. The overlay is shown in Figure 3. The overlay was placed on the aperture chart, and the number of increments of each intensity is counted in each Fresnel region. The displacement between the center of the overlay and the center of the aperture is scaled to measure the angular displacement of the test point from the axis of the beam. Figure 4 displays the overlay on the center of the beam and Figure 5 shows the overlay displaced the equivalent of 5.30 degrees from the beam.

For computation on or near the center of the main beam, where the first and other low order Fresnel regions are involved, the phase distribution in the region was considered. However, at displacements from the axis of the main beam such that higher order Fresnel zones are predominant, phase relations in the zones were assumed to integrate out.

The results obtained from the analogue method are listed in Table I:

Table 1

Illumination Taper	Edge To Center Power Ratio	Range	Angle Off Axis	Power Ratio To Axis At 4,000 Feet	Milliwatts Per Square Centimeter (10 KW Trans.)
$\left(1 - \frac{r^2}{R^2}\right)^{\circ}$	0 db	400 ft.	0.0°	23.56	31.60
$\left(1 - \frac{r^2}{R_1^2}\right)$	-10 db	400 ft.	0.0°	35.35	47.38
$\left(1 - \frac{r^2}{R_2^2}\right)$	-20 db	400 ft.	0.0°	43.17	57.87
$\left(1 - \frac{r^2}{R^2}\right)$	-α db	400 ft.	0.0°	48.32	64.77
$\left(1 - \frac{r^2}{R^2}\right)$	-α db	400 ft.	5.3°	0.11	0.147
$\left(1 - \frac{r^2}{R^2}\right)$	-α db	4000 ft.	0.0°	1.00	1.34

The illumination taper with 10 db and 20 db edge power level was accomplished mathematically by extending the radius of the aperture artificially to R_1 and R_2 such that the power level at the true radius R was -10 db or -20 db according to the relation:

$$\text{Energy Ration} = 1 - \left(\frac{r^2}{R_1^2}\right)^2$$

Here, r is the distance from the center of the aperture and R_1 is an artificial aperture diameter which produces a 10 db energy level at the edge of the true aperture. Figure 6 is a graph of the electric intensity for zero, -20 db, and -10 db edge illumination. Figure 7 is a bar graph showing how the energy is distributed along the radius of an aperture illuminated by a $\left(1 - r^2/R^2\right)$ taper.

b. Graphical Solutions

At this time we were able to obtain a copy of a new book (Reference 1) which had information pertinent to the subject of near field. Volume One, "Microwave Scanning Antennas", edited by R. C. Hansen, discusses the near field in the first chapter.

By consulting two curves in the chapter, and by making the necessary coordinate conversions, it is possible to estimate the near field intensity for a point at 400 feet range and 5.3° off the axis.

On page 29, (Reference 1), curves are given for the near field intensity for an aperture with a diameter of 10λ. This aperture is illuminated by a 25 db circular field with Taylor distribution. Based upon these curves, a curve is developed in Figure 8 with the coordinates changed to correspond to our aperture, that is, an aperture which has a diameter of 66.7λ. Since we are concerned with the area in the proximity of the point under study, the envelope of peak values should be used. To develop the curve in Figure 8 from the curves in Reference 1, the envelope of the peak values for $\Delta = 0.75$ was constructed. A similar envelope for peak values for $\Delta = 1.25$ was drawn. Figure 8, which represents the envelope for $\Delta = 1.00$, was developed as the mean value of the envelopes for $\Delta = 0.75$ and $\Delta = 1.25$.

The Δ factor, shown on the graph, is the ratio of the range, L, of the point under study, to the range, L_1, of the transition point between the near and the far field. The range of the transition point, L_1, is given by

$$L_1 = \frac{2D^2}{\lambda}$$

and

$$\Delta = \frac{L}{L_1}$$

where:

L_1 = range to transition point

L = range to study point

D = diameter of aperture

λ = wave length

Δ = delta factor

For the 30-foot aperture at S-band L_1 = 4000 feet. Thus Δ, for the point in question (400 ft.), has the value 0.1.

For the above conditions, the curve in Figure 8 gives a field intensity ratio of 0.0316 between the 5.3° off axis point and a point on the axis at the same range. This is equivalent to a power ratio of $(0.0316)^2$, or 0.001.

It is now necessary to determine the relation between the power density at a point on the axis at a range of 4000 feet to the power density at a point on the axis at a range of 400 feet (Δ = 0.1). Figure 9, taken directly from Reference 1, page 38, Figure 22, is included here for the convenience of the reader. This curve indicates that the power density at a point on the axis at 400 feet range (Δ = 0.1) is forty one (41) times greater than the power density at a point on the axis at a range of 4000 feet (Δ = 1.0).

By combining the information taken from the two curves it is seen that the power density at a point 5.3° off the axis at a range of 400 feet is 0.041 times the power density at a point on the axis at 4000 feet range.

If the power density at 4000 feet on the axis is 1.34 watts per square centimeter, the power density at 5.3° off the axis at 400 feet range is 0.055 watts per square centimeter.

Although there is ample mathematical slack, in the two methods employed to account for the difference in the results (0.147 m. w. per sq cm for the analogue method and 0.055 m. w. per sq cm for the curves) it was decided that a more exacting computation should be made.

c. Analytical Methods

A search of current literature, with the assistance of the reference list in the "Microwave Scanning Antenna" book (Reference 1) disclosed a paper entitled "Fresnel Region Fields of Circular Aperture Antennas" (Reference 2) by Ming-Kuei Hu, published in 1961.

The method for computing near field intensity, developed in this paper involves two approximations. First, the Newton iteration formula for the square root of a number is used; and second, the cosine of the angle off axis must be close to unity. Also the product of the radius of the aperture times the sine of the off axis angle must be small relative to the range of the computation point.

Within the foregoing limitations, Hu has developed a solution for the field intensity in terms of Lommel's functions for two variables. In his solution, the two variables are γ and u, defined as follows:

$$\gamma = \frac{Ka}{r}$$

$$u = Ka \sin \theta$$

where

$$K = \frac{2\pi}{\lambda}$$

λ = wave length of transmission

a = radius of the aperture

r = range to computation point

θ = angle between the axis and a line from the aperture center to the computation point

The situation is complicated by the necessity to use hand computational methods for the solutions. Unfortunately, available tables of Lommel's Functions (Reference 3) are very restricted and include only a few values which are of immediate interest. Table 2 is a listing of the Lommel Functions used. Hu, in Reference 2, indicates a method for deriving Lommel Functions from Bessel Functions. The method involves a series in Bessel Functions, and in most cases, required about twenty terms for convergence. Also available Bessel Function Tables (Reference 4) do not go beyond argument 29, thus restricting computation to angles of less than 8.2° (u = 29) from the axis of the beam. This latter limitation is not serious since the topography calls for an evaluation in the proximity of 8 degrees off the axis.

The Lommel Functions with argument 8.00 order 7.584 which were available in the tables, were computed by series for comparison with values found in the tables. This serves as a check on the function computational method. The agreement is satisfactory since the Bessel Functions are given to only four places.

Table 2
Values for Lommel Functions

Order	Argument	Tables		Computed	
		U_1	U_2	U_1	U_2
0.7584	0.00			+0.370177	+0.071039
7.5840	0.00			-0.608386	+1.796154
15.6800	0.00			+0.963770	+0.733290
6.0674	1.00			-0.060490	+1.761240
7.584	1.00			-0.068000	+1.516400
6.067	8.00	+0.309245	+0.010907		
7.584	8.00	+0.457602	+0.113549	+0.457453	+0.113833
7.584	19.00			-0.046523	-0.030498
7.584	20.00			+0.032149	-0.025883
7.584	27.00			+0.041894	-0.005110
7.584	28.00			+0.037866	+0.006693
15.168	28.00			+0.093669	+0.038384
7.584	29.00			+0.001487	+0.010864
15.168	29.00			-0.002102	+0.054380

The paper prepared by Hu, (Reference 2), presents methods for the solution of circular apertures with uniform illumination. The solution for the tapered illumination involved the differential of the Lommel Functions. In view of the necessary differentials and also since there is not much difference in the field intensity, for relatively large off axis angles (8° to 10°), between uniform and tapered illumination, it was decided to make the computations for uniform illumination of the aperture.

It should be observed that the attenuation along the beam axis for an aperture of uniform illumination is considerably different from the attenuation along the beam axis for a tapered illumination.

Since maximum probable values are desired for this computation, the attenuation along the axis will be taken for a tapered illumination, as shown in Reference 1 and the attenuation due to displacement from the axis will be computed for uniform illumination. The results of the computations are shown in Table 3.

Although not directly applicable to the immediate problem, some computations were made at a range of 500 feet to check the computations against the corresponding data from Reference 2. The 500 foot range is equivalent to a value of 1.25, and is plotted on curve 6, Figure 5 of Reference 2. The ratio

Table 3
Computed Power Density

Range (Ft.)	Angle Off Axis (Deg)	U	Ratio Field On Axis To Field Off Axis	Power Density Ratio On Axis To Off Axis	Power Density Ratio To On Axis At 4000 Ft.	Computed Milliwatts Per Sq Cm From 10 KW	Power Density With Tapered Illumination From 10 KW
500	0.2834	1	0.8900				
500	2.2670	8					
4000	0.0	0				1.340	1.340
400	0.0	0			25.311	33.90	55.940
400	0.2834	1	0.8762	0.7677	19.432	26.04	42.970
400	2.2670	8	0.2488	0.0619	1.567	2.010	3.320
400	5.385	19	0.0293	0.00086	0.0217	0.029	0.048
400	5.668	20	0.0218	0.00005	0.0120	0.016	0.026
400	7.652	27	0.0223	0.00050	0.0125	0.017	0.028
400	7.935	28	0.0203	0.00041	0.0104	0.014	0.023
400	8.219	29	0.0058	0.000033	0.00085	0.0011	0.0019
200	0.0	0			10.325	13.863	44.220
200	7.935	28	0.0836	0.0070	0.0724	0.097	0.314
200	8.219	29	0.0449	0.0020	0.0247	0.033	0.107

of the field intensity at $u = 1$ to the field intensity at $u = 8$ from the curve is 5.40. The ratio for the same two points as computed is 5.70. This difference can be accounted for by a slight laxity in curve plotting.

The energy density at 4000 feet range ($\Delta = 1$) is computed in the usual manner, using the specified gain of the antenna (44 db) and the maximum power input of 10 kilowatts. The computations for the on axis field intensity ($u = 0$) required an evaluation of the Lommel Function at $u = 0$. This in turn required the Bessel Functions $U_n(0)$. Although these values do not appear in Jahnke and Emde, it was pointed out by Dr. F. O. Vonbun that the values for $U_n(0)$ divided by γ^n could be computed from the series solution for the Bessel Functions given in Jahnke and Emde.

Field intensity ratios were computed for all values listed in Table 3 by the method described by Ming-Kuei Hu in his paper on Fresnel Region Fields of Circular Aperture Antennas, (Reference 2), for the case of uniform aperture illumination.

The last column in Table 3 is the energy density at the specified point in space when the attenuation along the beam is taken from the curve on Figure 9 and the attenuation off the axis is computed by the method given by Hu in Reference 2. This procedure gives the highest value for the power density since attenuation along the beam is less for tapered illumination and attenuation off the axis is less for uniform illumination. It is felt that more exact and possibly slightly lower values for the power density could be obtained by use of the taper illumination methods discussed by Hu in his paper, however, the computations involved are long and tedious by hand. The energy density data from Table 3 is plotted in Figure 10. This curve represents the envelope of the peak values of the energy density from the 30-foot S-band antenna when transmission is 10 KW. The solid curve is for a range of 400 feet and the dotted curve is for a range of 200 feet. For comparison, the points computed by the analogue and the graphical methods are spotted on this curve.

II. COMPARISON WITH EXPERIMENTAL RESULTS

a. Radar Data

It is further desired to check the results given by Hu against experimental results. Some test data on the AN/FPQ-6 Radar is given in an RCA report "Missile Precision Instrumentation Radar Set AN/FPQ-6 (Reference 5). Figure 11 is a graph of relative energy density taken directly from Reference 5. This curve includes a plot of the single lobe antenna pattern, and the dual lobe simultaneous lobe pattern. Since the single lobe pattern is used in transmission mode, this report is concerned only with the single lobe pattern. Table 4 is developed from the information in Figure 11.

Table 4

Experimental Data for AN/FPQ-6 Radar

Angle From Axis	db Down	Power Ratio	Field Intensity Ratio	U
0.00°	0	1.0000	1.0000	0.000
0.50°	-34	0.0004	0.0200	4.528
0.65°	-18	0.0159	0.1260	6.173
0.90°	-30	0.0010	0.0316	9.266
1.02°	-24.5	0.0036	0.0600	11.973
1.32°	-31.5	0.0007	0.0270	12.910

Knowledge of the illumination taper used on the FPQ-6 is not availabel in the office. However, an examination of the position of the peaks and nulls given in the paper by Hu, suggests that the illumination taper lies between $(1-\rho^2)^0$ and $(1-\rho^2)^1$.

Table 5 gives the position of the peaks and nulls, as shown in Figures 5 and 6 from Reference 2.

Also shown in Table 5 is the average value for the position of the peaks and nulls for the two conditions of illumination, and the average field intensity for the nulls and peaks.

Table 5
Data From Figure 5 and Figure 6, Reference 2

	U For $(1-\rho^2)^0$ Illum	U For $(1-\rho^2)^1$ Illum	Eθ For $(1-\rho^2)^0$ Illum	Eθ For $(1-\rho^2)^1$ Illum	Average (Col. 1 & 2)	Average (Col. 3 & 4)
axis	0.00	0.00	1.000	1.000	0.00	1.000
1st null	3.85	5.15	0.090	0.060	4.50	0.075
1st peak	5.10	6.30	0.145	0.075	5.70	0.110
2nd null	7.05	8.20	0.020	0.000	7.63	0.010
2nd peak	8.50	10.00	0.060	0.025	9.25	0.043
3rd null	10.10	12.00+	0.016	0.000	11.05+	0.007

The average position of the peaks and nulls given in Table 5 is in good agreement with the position of the peaks and nulls given in Table 4. The peak field intensity values are in good agreement, but, as may be expected, some considerable divergence is present in the null values.

III. CONCLUSIONS

The solution for the off beam intensity in the near field, like nearly all complex engineering problems, does not lend itself readily to an analytical solution. Likewise, it is not readily adopted to the usual automatic computing equipment which is basically designed for the solution of bookkeeping problems.

It can be seen that the assumptions made for the analytical solution followed here limit the magnitude of the "off beam" angle. The extent to which the accuracy of the solution deteriorates with increase in "off beam" angle has not been investigated. It is consoling to observe that the points computed by the analogue

and the graphical methods are in good agreement with the analytical solution. (The graphical method is an extension of other analytical solutions which make other approximations.)

The analogue method entertains the greatest potential for a more accurate solution of this problem, provided a suitable machine program could be devised for the adaptation to existing machines. If, however, a good engineering computing machine were available, say a DDA-GP combination, a more suitable and adaptive analogue could be constructed. An improved analogue could include the obstruction due to the feeder system. The analogue used here was devised for hand solution.

It should be remembered that the computations and these results are concerned only with the radiation from the main aperture. Other sources of energy may be present. These include:

(a) Energy leaking around the edge of the sub reflector of the Cassegranian System.

(b) Energy leaking over the edge of the parabolic reflector.

(c) Energy reflected from the feeder system and supports.

(d) Energy reflected from the ground or from structures in the proximity of the antenna.

The computations show that a field energy density of less than one milliwatt per square centimeter may be expected at angles of more than four degrees from the axis of the beam at a distance of 400 feet from the 30-foot S-band antenna with a 10 KW transmission level. Under similar conditions, the field energy level will be less than one milliwatt per square centimeter for angles of more than eight degrees from the beam axis at a range of 200 feet from the aperture.

However, suppression of side lobe energy must be taken into consideration in all phases of the design of the feed system. The configuration of the horn, or primary emitter, and the subreflector must be such that the illumination taper on the main reflector approaches zero at the edge. The taper design must take into consideration the energy level in the remote side lobes as well as those lobes in the immediate proximity of the main beam.

Care must also be exercised to insure that leakage around the edge of the subreflector, and over the edge of the main reflector does not result in field intensities greatly in excess of the aperture side lobe intensities computed in this report.

ACKNOWLEDGMENTS

The author wishes to express his appreciation to Dr. F. O. Vonbun for reviewing this work and for the helpful suggestions offered during the preparation of the report. Also, the technical information provided by Mr. Anthony Grandinetti and Mr. Severino Santos, of Manned Flight Engineering Branch, is appreciated.

REFERENCES

1. "Microwave Scanning Antennas." Volume 1, Academic Press 1964. Edited by R. C. Hansen

2. "Fresnel Region Fields of Circular Aperture Antennas," by Ming-Kuei Hu. Journal of Research of the National Bureau of Standards, Vol. 65D No. 2, March-April 1961.

3. "Lommel Functions of Two Variables." E. N. Dekanosidze. Translated from Russian by D. G. Fry, Pergamen Press, 1960.

4. "Tables of Higher Functions." Jahnke-Emde-Losch. McGraw-Hill Book Co., Sixth Edition, 1960.

5. "MIPIR Final Report." Missile Precision Instrumentation Set AN/FPQ-6. RCA Report.

6. "Design Analysis—Unified S-Band System for Apollo Network," Volume 1 Parts I and II. Collins Radio Company Engineering Report. Oct. 28, 1964.

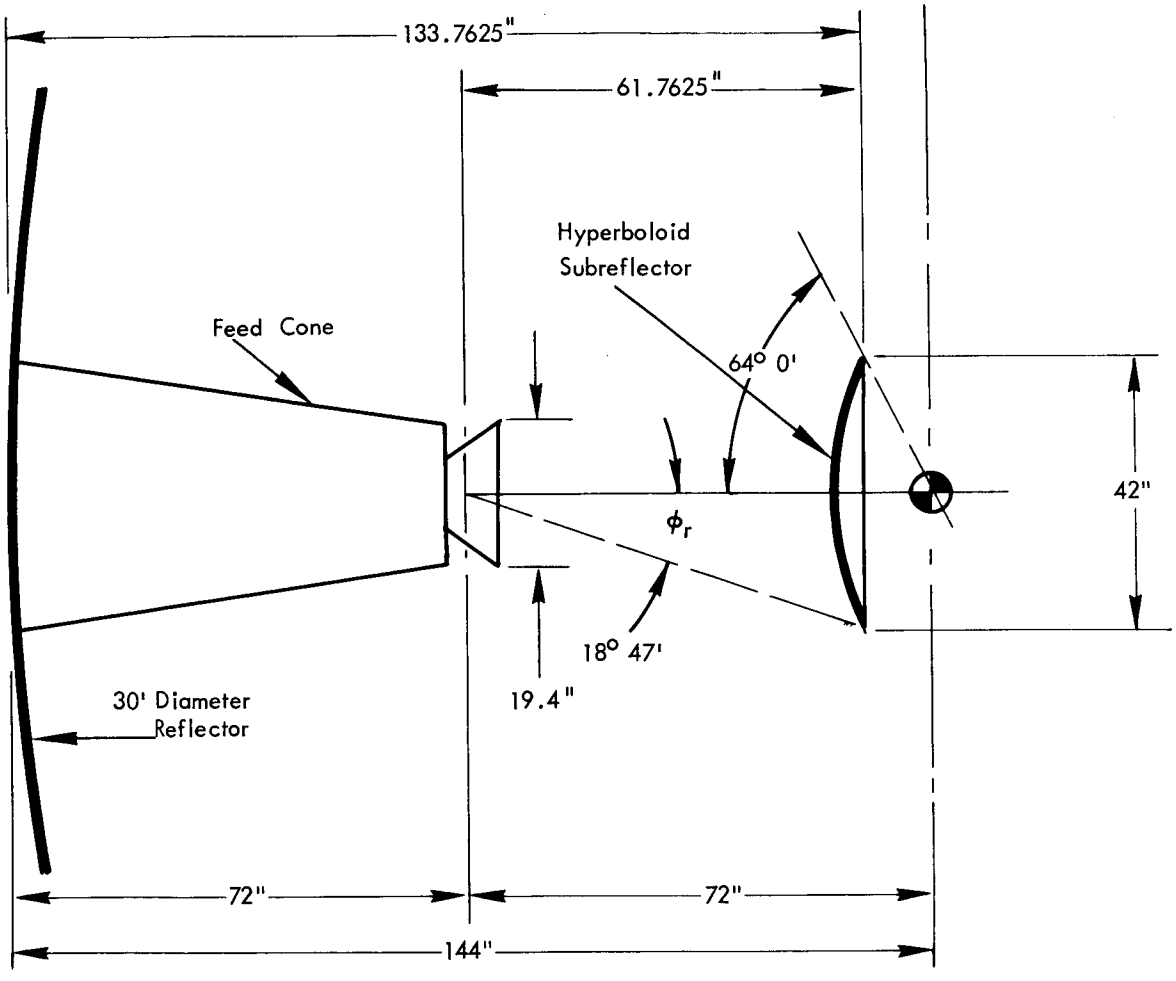

Figure 1—Dimensions of S-Band Feeder System Proposed by Collins Radio Company.

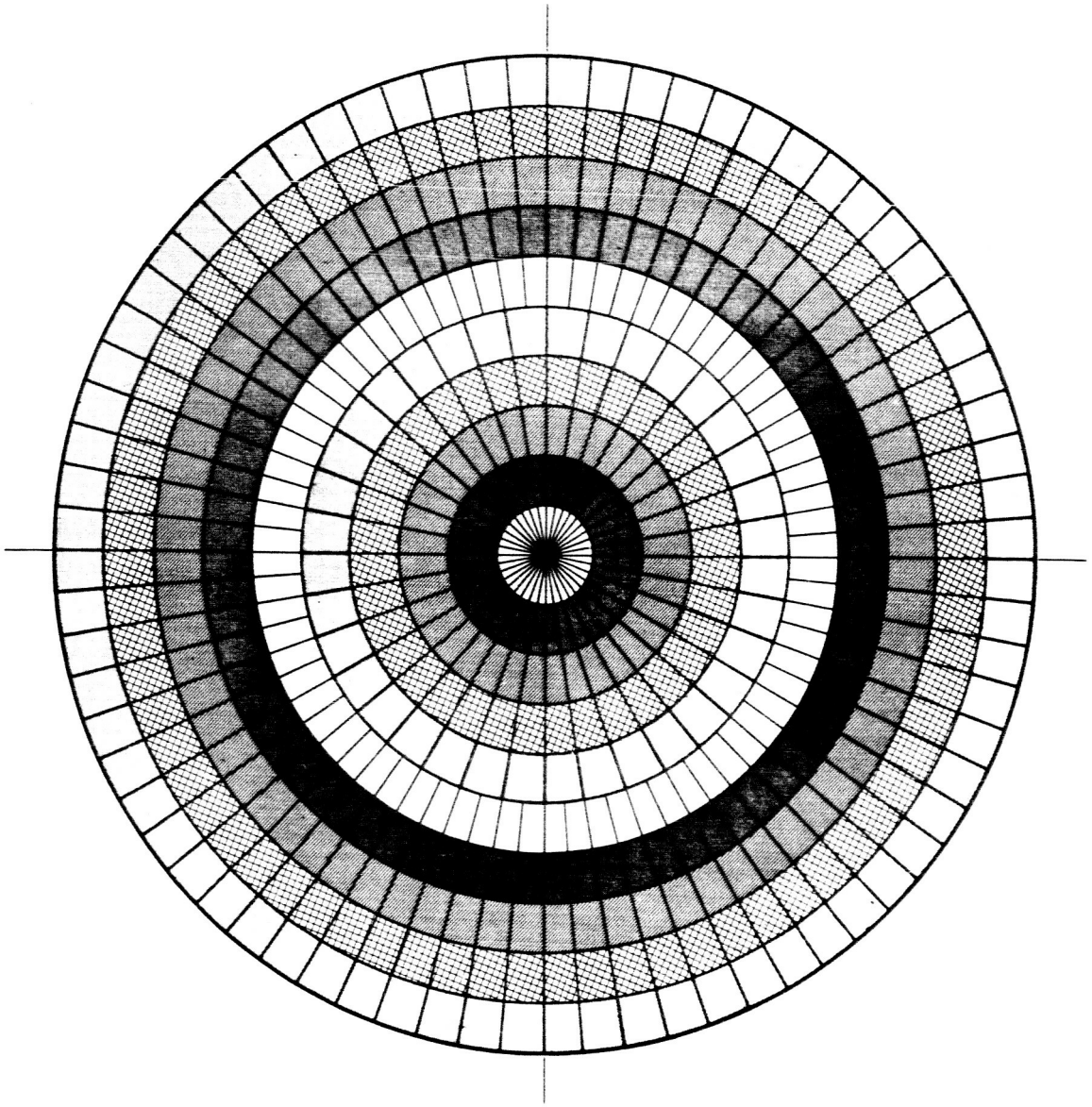

Figure 2—Circle with Coded Bands Indicating Distribution of Energy Density.

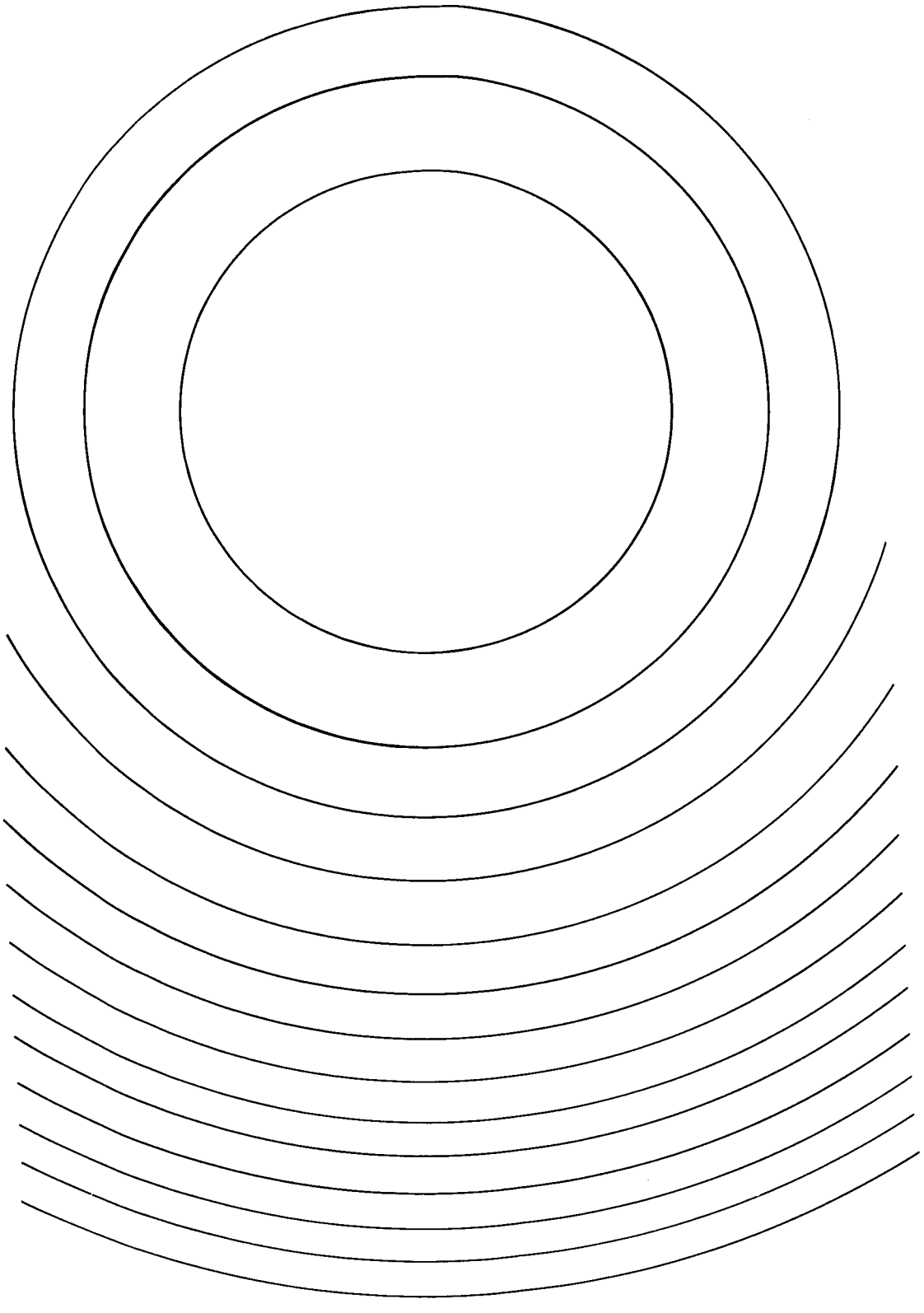

Figure 3—Transparent Overlay with Circles Indicating Boundaries of Fresnel Regions. Scaled to Figure 2, with 400 Foot Range and λ = 0.450 Ft.

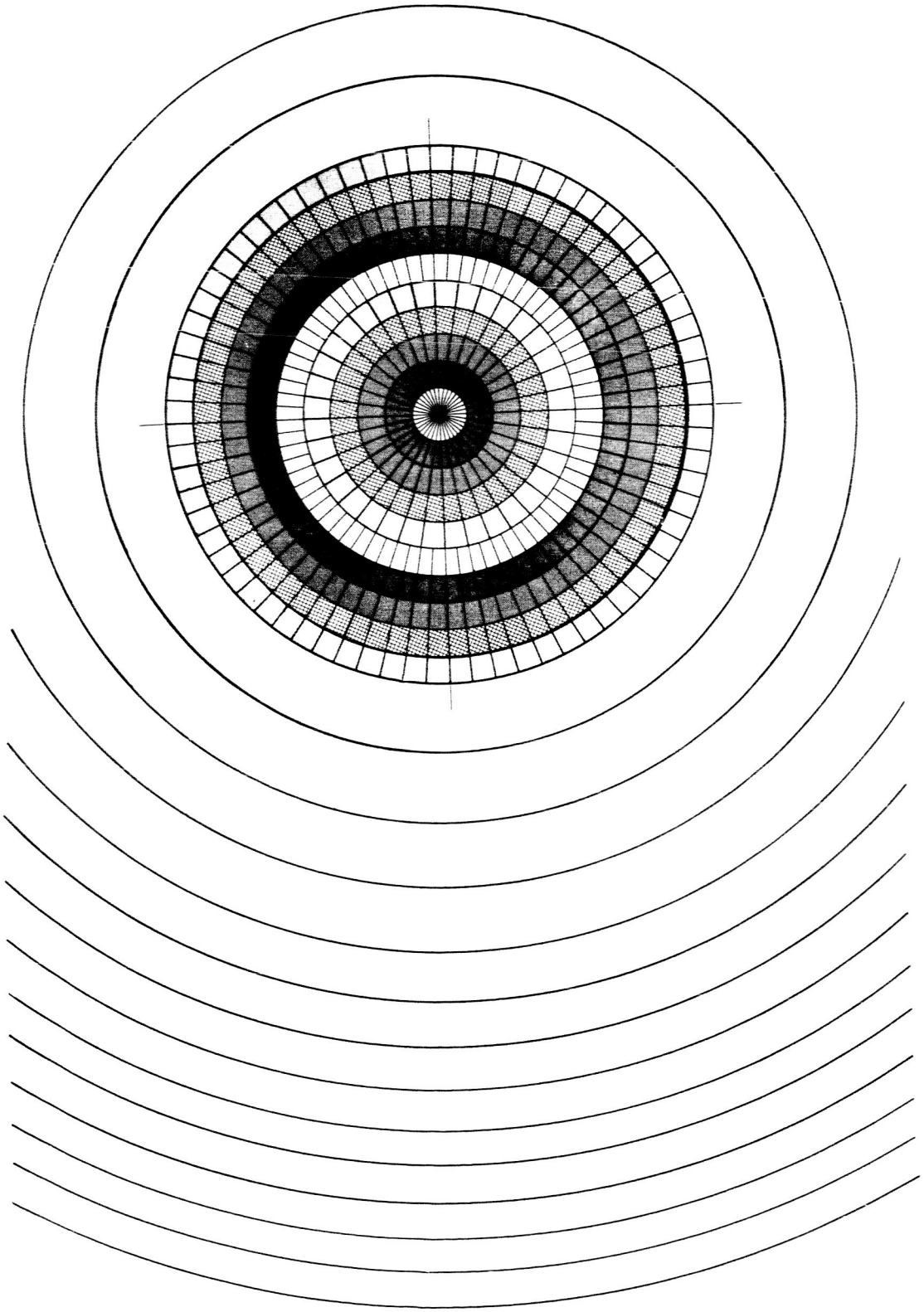

Figure 4—Overlay on Figure 2 for Position on Axis of Transmitted Beam.

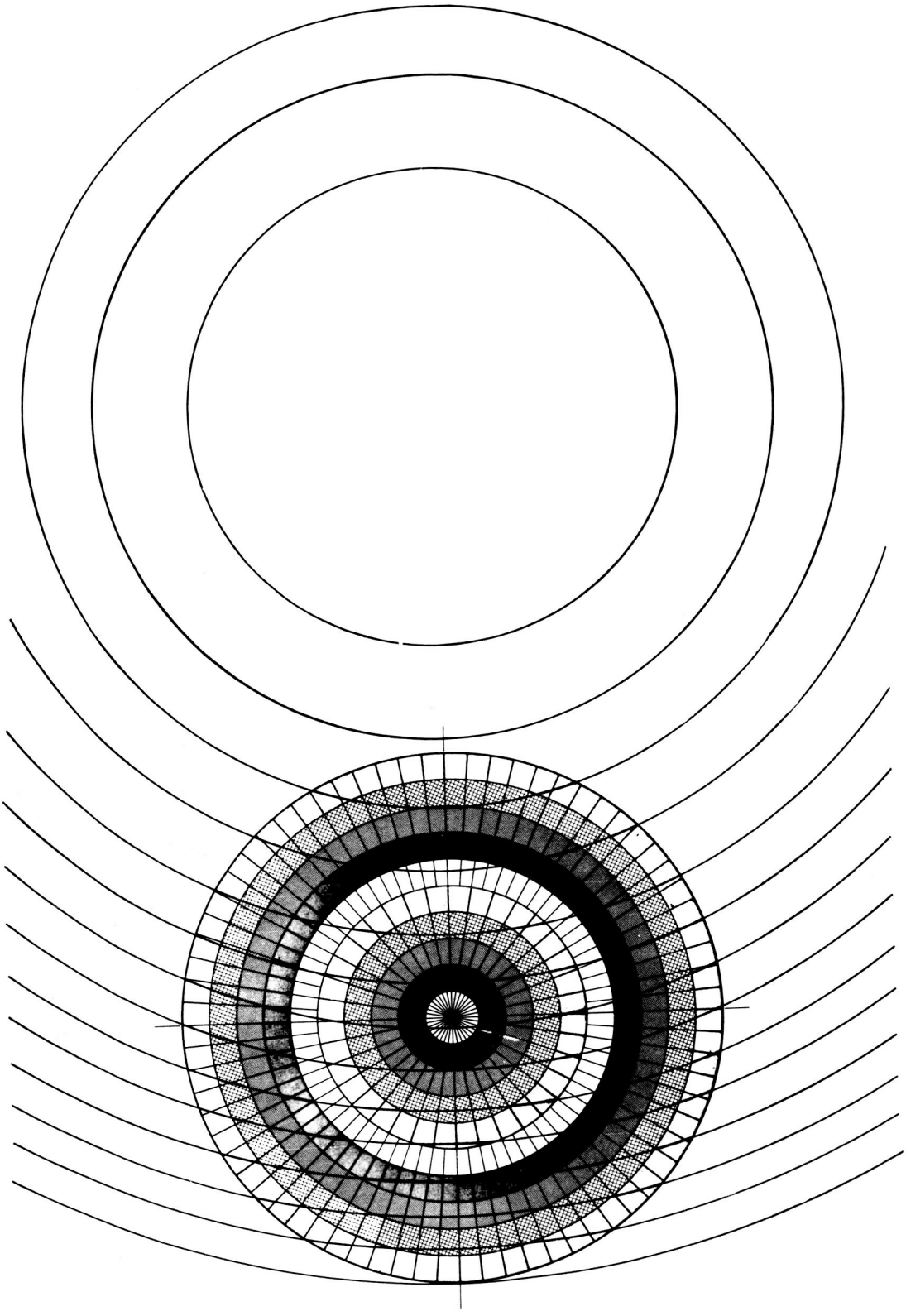

Figure 5—Overlay on Figure 2 for Position Displaced 5.3 from Axis of Beam.

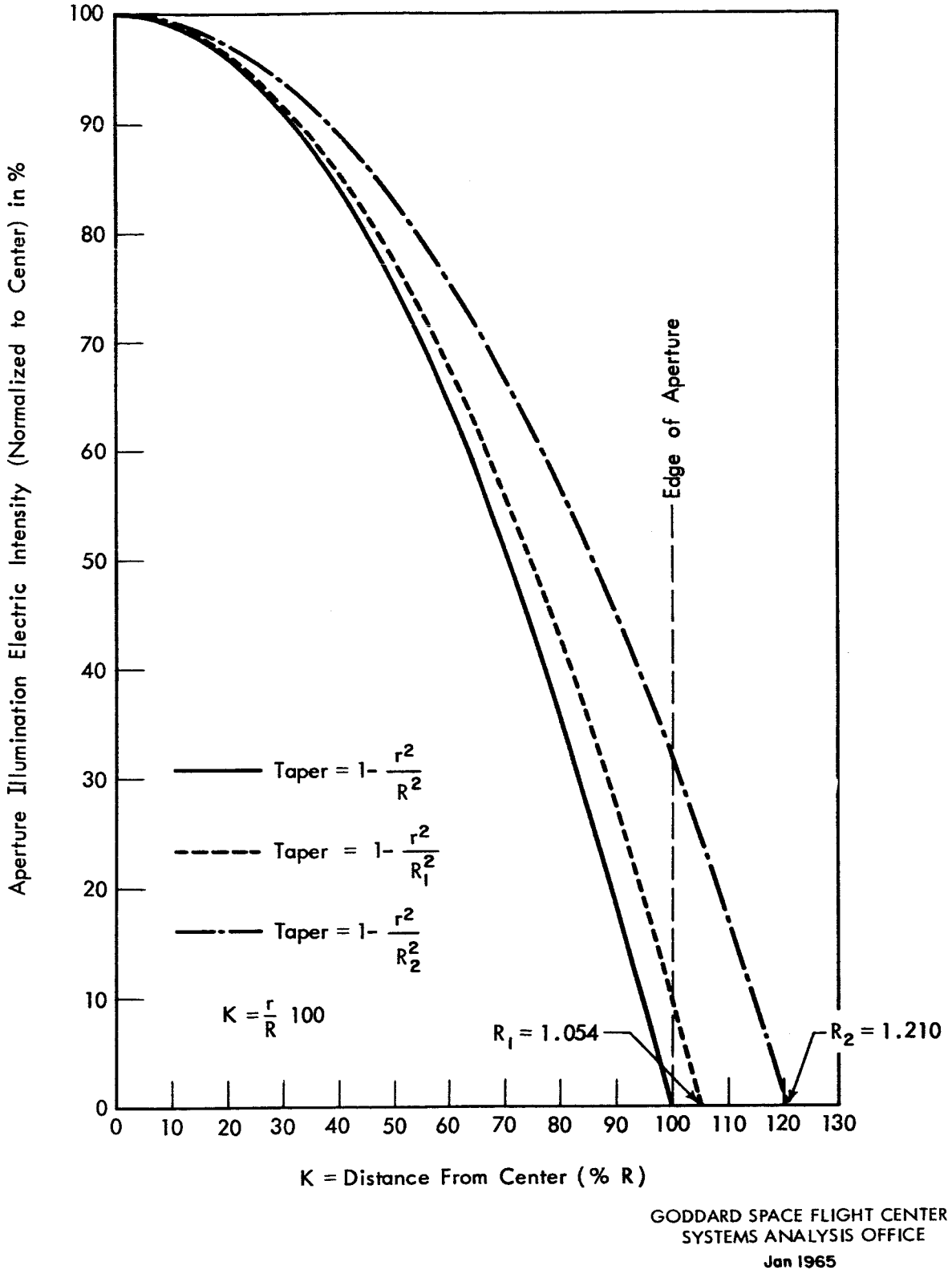

Figure 6—Distribution of Electric Intensity over Aperture.

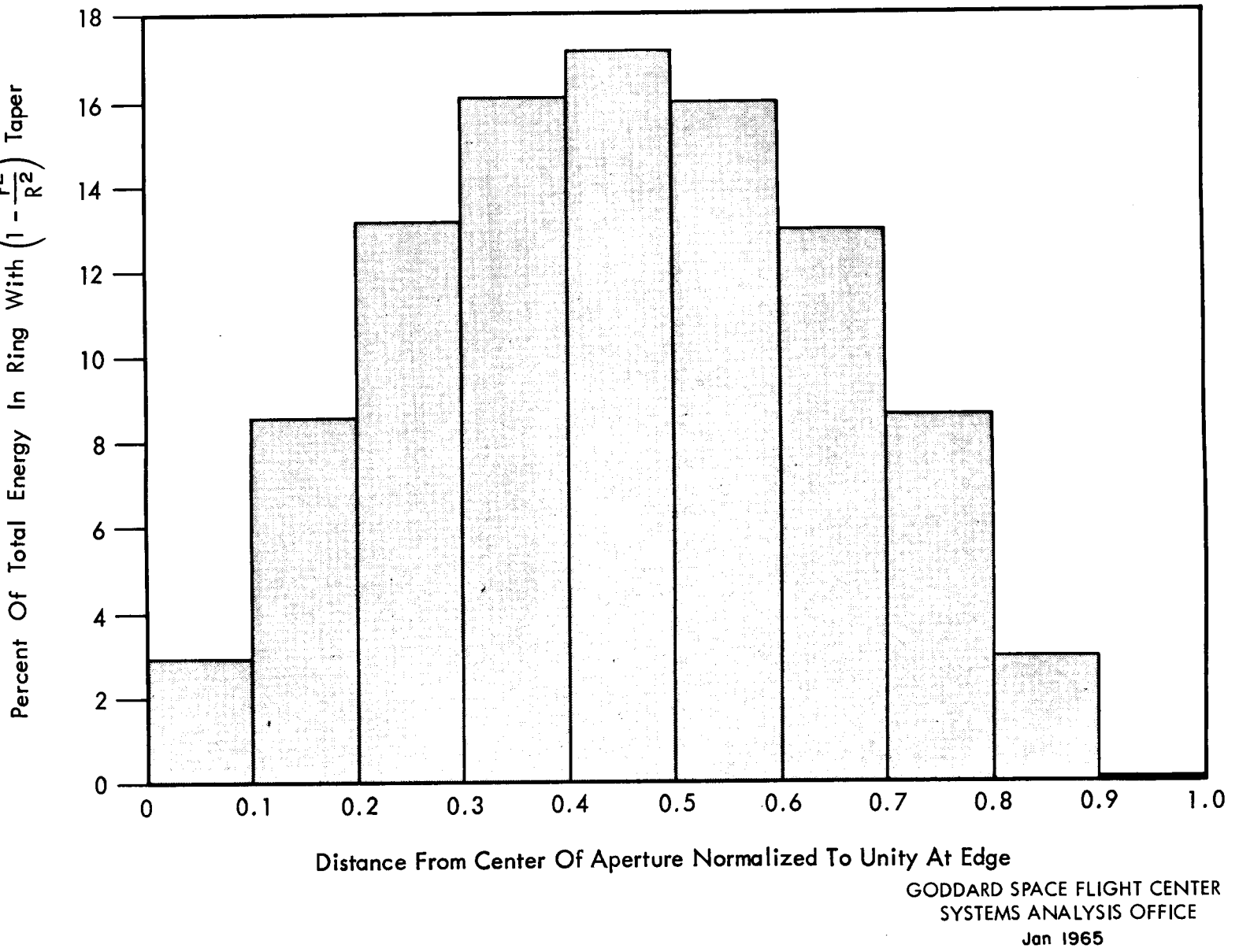

Figure 7—Bar Graph, Distribution of Energy with Radius of Aperture.

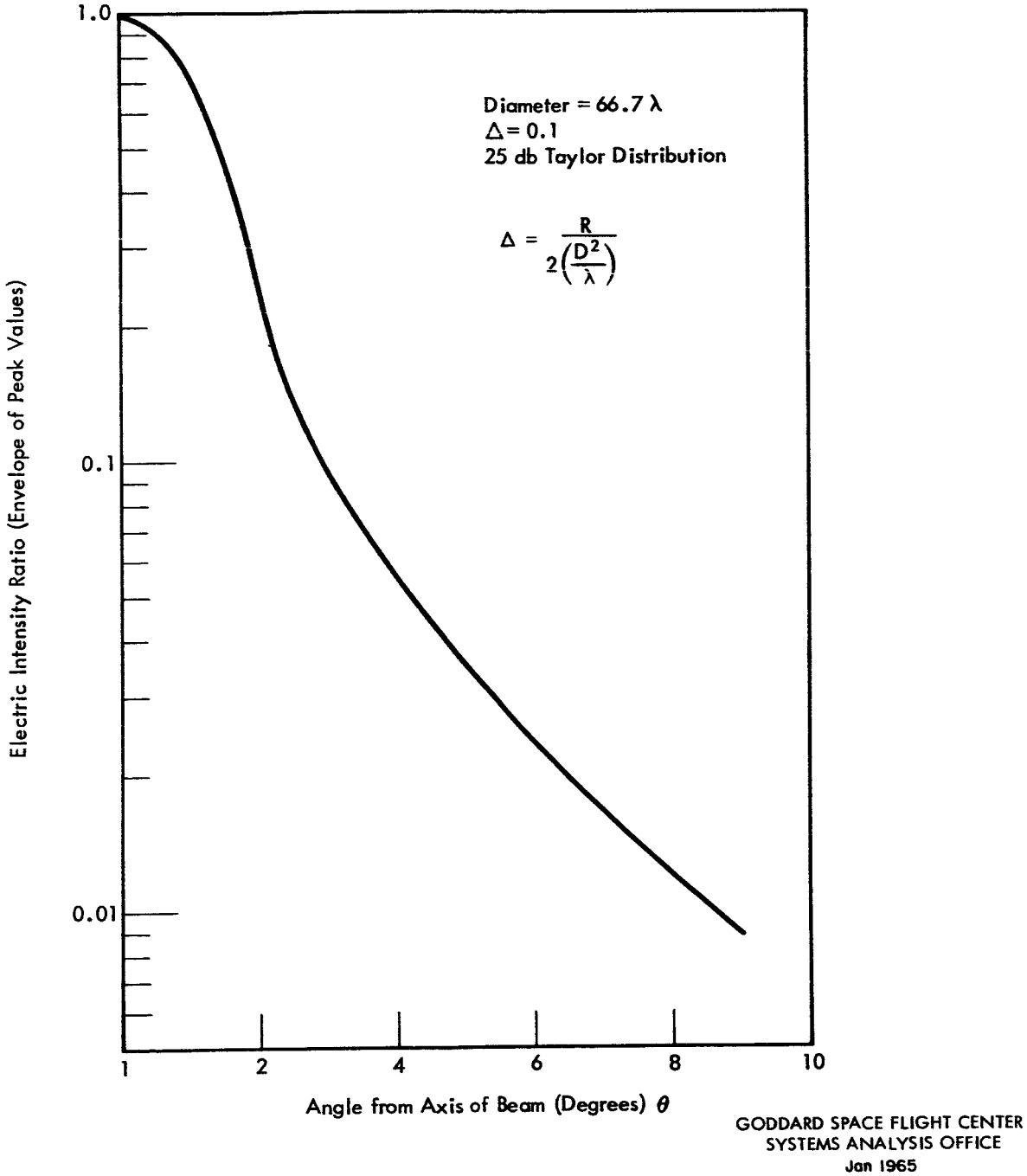

Figure 8—Envelope of Peak Side Lobe Electric Intensity for $\Delta = 0.1$ Normalized to Unity on the Axis of the Beam.

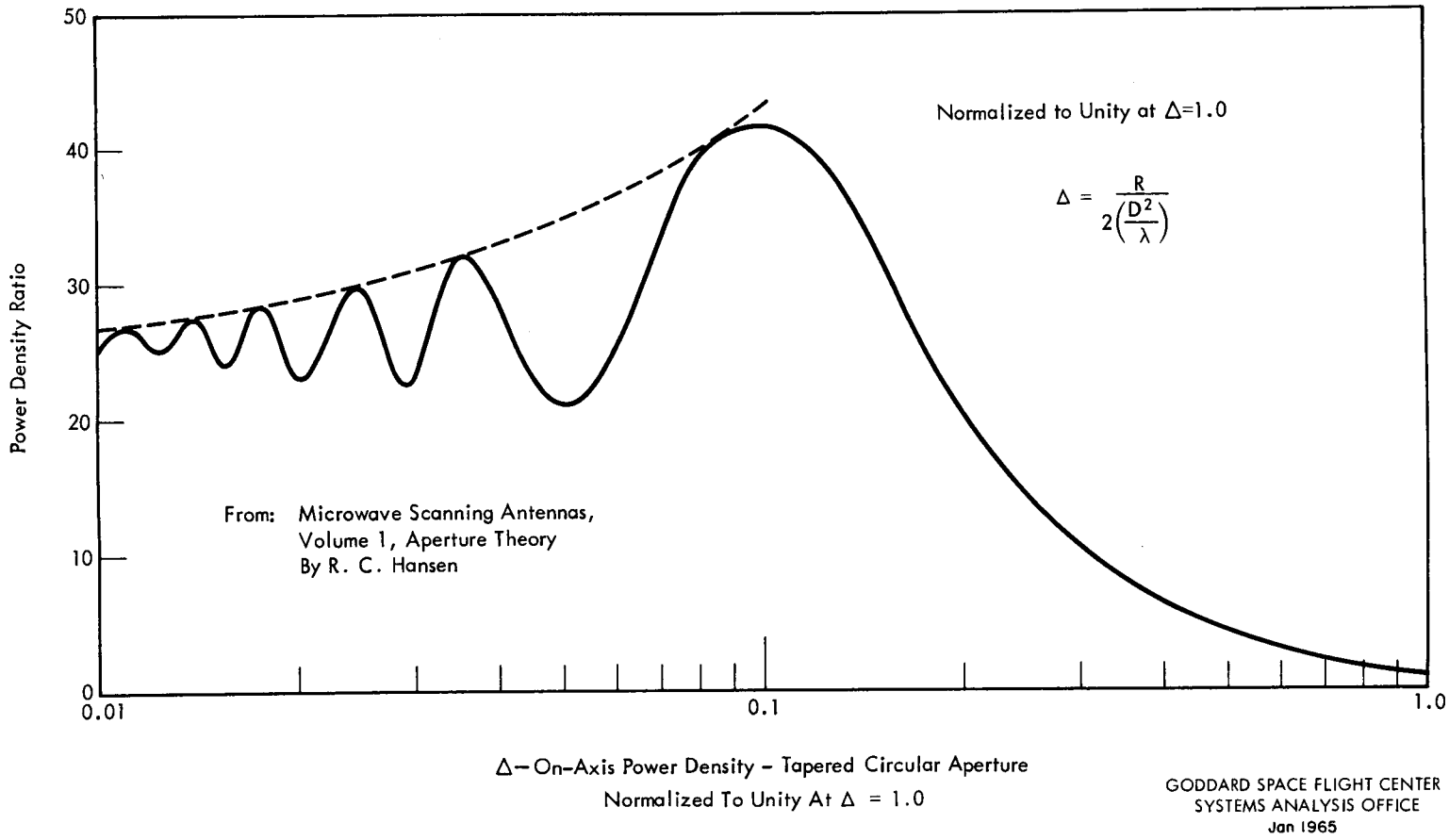

Figure 9—On Axis Power Density Ratio.

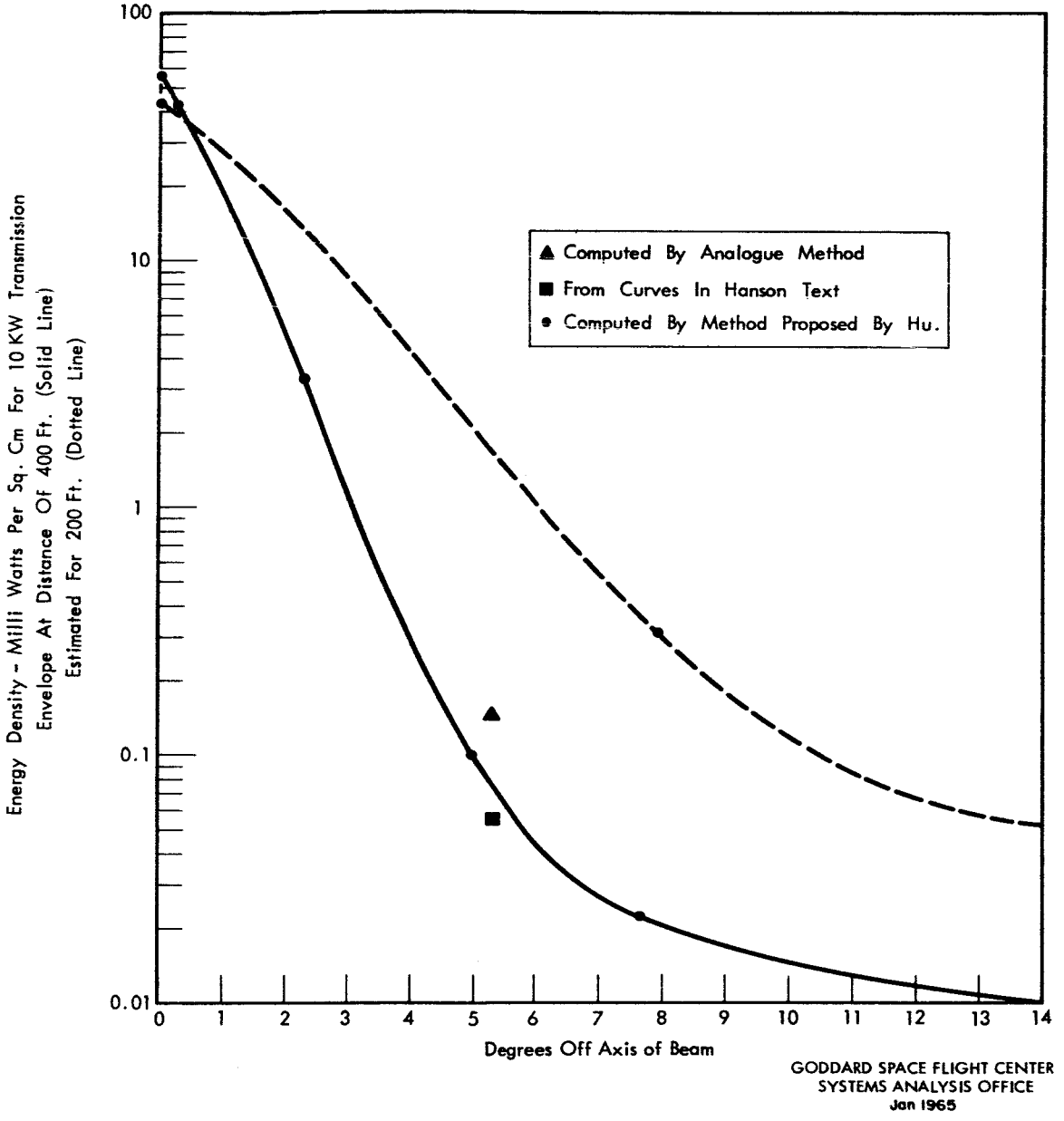

Figure 10—Curve 1 - Envelope of Energy Density in Near Field of 30-Foot S-Band Antenna with 10 KW Transmission Computed Nov. 1964. SAD - GSFC.

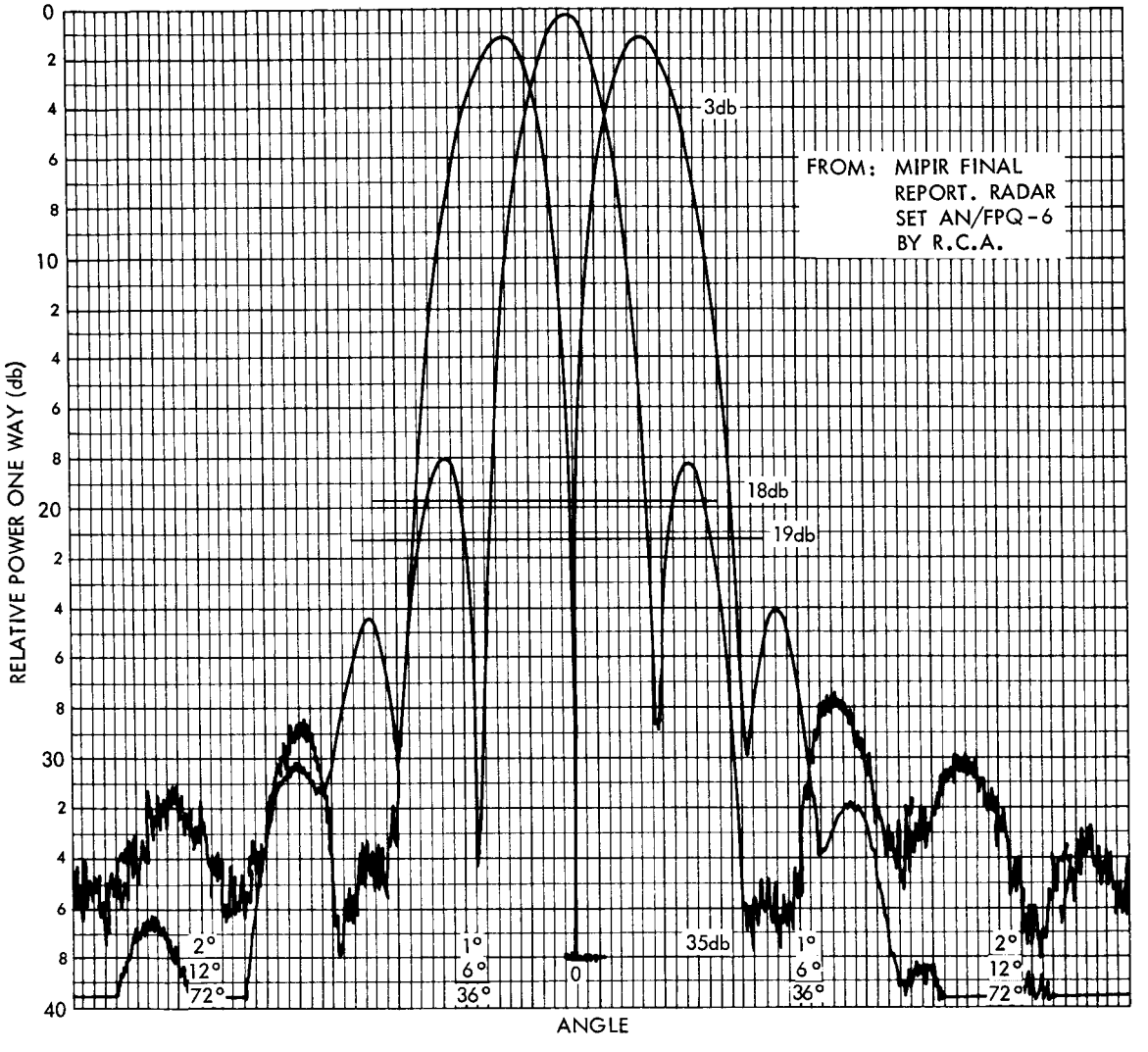

Figure 11—Antenna Pattern Test Data from AN/FPQ-6 Radar Set.